Evidence suggesting that earth had a ring in the Ordovician

Andrew G. Tomkins [*], Erin L. Martin, Peter A. Cawood

School of Earth, Atmosphere and Environment, Monash University, Melbourne, Victoria 3800, Australia

ARTICLE INFO

ABSTRACT

All large planets in our Solar System have rings, and it has been suggested that Mars may have had a ring in the past. This raises the question of whether Earth also had a ring in the past. Here, we examine the paleolatitudes of 21 asteroid impact craters from an anomalous ~40 m.y. period of enhanced meteor impact cratering known as the Ordovician impact spike, and find that all craters fall in an equatorial band at $\leq 30°$, despite ~70 % of exposed, potentially crater-preserving crust lying outside this band. The beginning of this period is marked by a large increase in L chondrite material accumulated in sedimentary rocks at 465.76 ± 0.30 Ma, which, together with the impact spike, has long been suggested to result from break-up of the L chondrite parent body in the asteroid belt. Our binomial probability calculation indicates that it is highly unlikely that the observed crater distribution was produced by bolides on orbits directly from the asteroid belt ($P = 4 \times 10^{-8}$). We therefore propose that instead, a large fragment of the L chondrite parent body broke up due to tidal forces during a near-miss encounter with the Earth at ~466 Ma. Given the longevity of the impact spike and sediment-hosted L chondrite debris accumulation, we suggest that a debris ring formed after this break up event, from which material deorbited to produce the observed crater distribution. We further speculate that shading of Earth by this ring may have triggered cooling into the Hirnantian global icehouse period.

1. Introduction

Interactions between the Earth and incoming materials from the Solar System have dramatically influenced the evolution of life on Earth, well exemplified by the extinction of the dinosaurs caused by the Chicxulub impact event (Alvarez et al., 1980; Hildebrand et al., 1991; Kring and Boynton, 1992). Unique in at least the last 540 m.y. (the period for which there are data; Terfelt and Schmitz, 2021), was a dramatic increase in the impact cratering rate and flux of meteorite material to Earth starting in the mid-Ordovician and extending for perhaps as much as 40 m.y. (Fig. 1; Liao et al., 2020; Martin et al., 2018; Osinski et al., 2022; Schmieder and Kring, 2020; Terfelt and Schmitz, 2021), although the duration is presently poorly constrained. The beginning of this period is recorded in limestone, at multiple places around the world, recognised by a 2–3 order of magnitude enrichment in L chondrite meteorite and micrometeorite debris (Martin et al., 2018; Schmitz et al., 2022, 2001; Terfelt and Schmitz, 2021). A coincident period of enhanced seismic and tsunami activity, recognised through globally distributed megabreccia deposits, may be related (Parnell, 2009); although an alternative has been suggested by (Meinhold et al., 2011). This event may have promoted the Great Ordovician Biodiversification Event (Schmitz et al., 2008), after triggering a global icehouse (Schmitz et al., 2019). Deposition of L chondrite material in limestones at this time was suggested to have been caused by an increase in asteroid dust dispersed throughout the inner Solar System after impact-associated break-up of an L chondrite parent body (LCPB) within the asteroid belt (Schmitz et al., 2008, 2001). We hypothesise that instead, a large L chondrite asteroid had a near-miss encounter with the Earth at about 466 Ma, passing within the Roche limit, which caused the body to break-up and form a debris ring.

To investigate the possibility of a ring-forming event in the mid-Ordovician, we examined the paleolatitude positions (based on six tectonic plate reconstruction models; Domeier, 2016, 2018; Merdith et al., 2021; Scotese, 2016; Torsvik and Cocks, 2016; Torsvik et al., 2014) of the 21 meteorite impacts known to coincided with the enhanced Ordovician meteorite flux. The beginning of the period of interest is considered to be precisely defined by the age of volcanic ash layers in the meteorite-rich limestone at Thorsberg Quarry in Sweden, at 465.76 ± 0.30 Ma (Liao et al., 2020). The duration of the period of time from that point is poorly constrained, but is based on the observation that there is still above background L chondrite flux preserved in the geological record 40 m.y. later (Martin et al., 2018; Terfelt and Schmitz, 2021). We

---

then calculated the probability that the observed crater positions resulted from randomly distributed impact events across the globe, which would be expected if all impactors were derived from orbits in the asteroid belt (Rumpf et al., 2016), but not if they were derived from a single body that broke up during a close encounter with the Earth.

2. Methods and results

2.1. Paleogeographic reconstructions of the Ordovician impact record

Paleogeographic reconstructions were modelled in GPlates using all available global plate models for the Ordovician. The models used in this study are DOM16 (Domeier, 2016), DOM18 (Domeier, 2018), TOR14 (Torsvik et al., 2014), MER21 (Merdith et al., 2021), SCO16 (Scotese, 2016), and TC16 (Torsvik and Cocks, 2016). A detailed critical evaluation of these plate models in the context of this study is provided in Supplementary Material.

The measured age data and present-day latitude and longitude of Ordovician impacts were acquired from (Schmieder and Kring, 2020). The impact sites were georeferenced and loaded into Gplates (https ://www.gplates.org/; Müller et al., 2018) along with the rotation model and landmass/craton/continent files for the six models. The impacts were assigned a plate ID correlating with the landmass of its present-day coordinates and then the models reconstructed to the Ordovician. Paleolatitude versus time data for each impact, and for the major cratons, from 467 to 400 Ma were exported for each model. To compare the plate models, the paleolatitude versus time data were then compiled into line graphs for the period of 467–400 Ma (Fig. 2) and box plots for 467–450 Ma, which is the period of the impact spike prior to the Hirnantian Icehouse glaciation (Fig. 3).

Impact paleolatitude distributions for each plate model for 467–450 Ma were quantitatively compared using the Kruskal-Wallis H test to evaluate the null hypothesis that the means of the impact paleolatitude distributions from each model are equal. Analysis of variance assumptions (ANOVA) of normally distributed data with equal variance among distributions were not satisfied so the non-parametric test was preferred. Kruskal-Wallis indicated that there was a statistically significant

difference between sample means ($H(5) = 45.13542$, $p = 1.36 \times 10^{-8}$, Fig. 3) and the null hypothesis was rejected. As a p-value, or statistical significance, does not measure the size of an effect nor the importance of a result, a Post-hoc Dunn's test was carried out to identify pairs that failed to reject the null hypothesis at a significance level of $\alpha = 0.05$. Dunn's test revealed that SCO16 was statistically significantly different from the other models ($\alpha = 0.05$, Fig. 3).

2.2. Estimation of continental area capable of preserving an Ordovician impact crater

To investigate the probability that the observed impact crater distribution is non-random, and preferentially distributed closer to the equator, we calculated the continental surface area capable of preserving mid-Ordovician impact craters. Processes that hide or remove evidence of an impact crater include: (1) burial beneath more recent sediments or ice (such as Antarctica and Greenland), (2) erosion in response to uplift or because the impact was located in a mountainous area, and (3) tectonic overprinting. Thus, areas best suited to preservation of mid-Ordovician impact craters are Cambrian and older rocks situated on stable cratons that have not been tectonically disturbed.

A further issue is that regions situated close to the south pole during the Ordovician could be covered in ice, which could plausibly prevent preservation of particularly smaller impacts, as would be the case for Antarctica today. But ice sheet extent varies as a function of global temperature. At the beginning of the period of interest, the global temperature was likely warm enough for there to be no large ice sheets at the poles (Fig. 1), but the global temperature plummeted dramatically from about 463 to 444 Ma to what was briefly the coldest period in the last 540 m.y. (the Hirnantian Ice Age) (Scotese, 2021). From about 450 to 444 Ma what are now Africa and South America are thought to have been largely covered in an extensive ice sheet (Scotese, 2021), so it might be expected that these regions would not preserve impact structures during this period.

We used QGIS (https://www.qgis.org/) and geological datasets from the USGS to evaluate each continent individually and calculate the appropriate surface areas. Rocks of Cambrian age or older located on
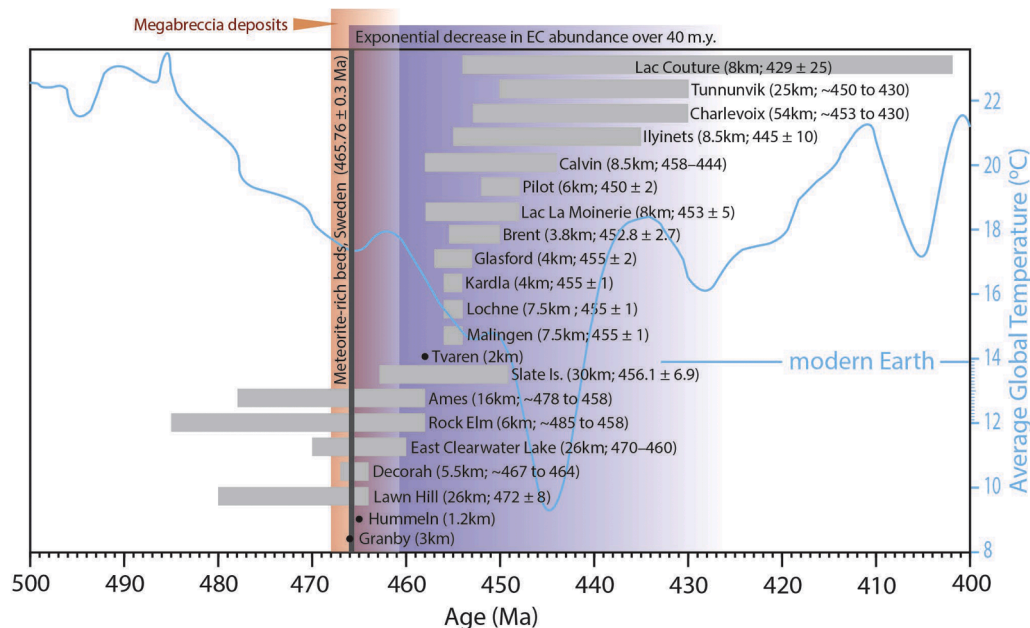

Fig. 1. Age estimates of the currently recognised Ordovician impact spike craters (Parisi et al., 2024; Schmieder and Kring, 2020), overlain on the estimated period of anomalous extraterrestrial chromite accumulation in sediments (Terfelt and Schmitz, 2021), and the known period of seismic/tsunami-induced megabreccia deposits (Parnell, 2009). The blue line indicates the global average temperature prior to 1990 (Martin et al., 2018; Schmitz et al., 2022; Scotese, 2021; Terfelt and Schmitz, 2021).
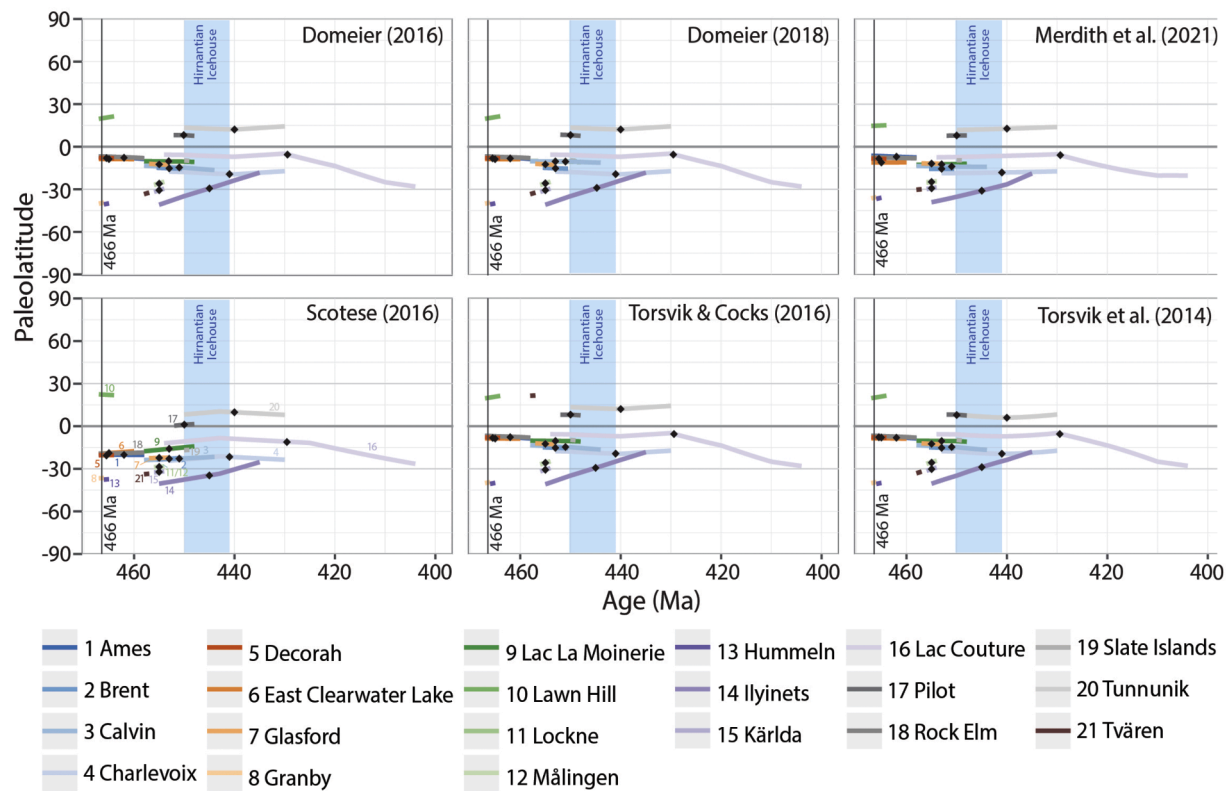
Fig. 2. Comparison of paleolatitude positions of the Ordovician impact craters for the six models evaluated. The length of each line represents the error on the age estimate, indicated by the point at the center.

stable cratons were included, and there are a small number of areas where minimally disturbed, flat-lying early Ordovician rocks could be included. Areas covered by younger material were removed from consideration; although advanced geophysical techniques and drilling can be used to locate and confirm shallowly buried impact craters, this approach has not yet been applied globally. Areas tectonised since the mid-Ordovician were removed from consideration. The depth of erosion since the mid-Ordovician is more difficult to evaluate on a global scale, but some areas in China were excluded because they have a combination of exposure of many younger granitoids (requiring erosion to expose) and recent tectonism to generate the granite magmas (further detail below).

Both Antarctica and Greenland were excluded because they are covered by ice today (the two craters identified under ice in Greenland have not been dated). The young tectonic elements in the Asia-Pacific are unsuited to preservation of Ordovician impact structures. The area estimates are based on the MER21 reconstruction for the period 466 to 450 Ma.

Australia. In Australasia, only the western two-thirds of Australia (west of the Tasman Line) is well suited to preservation of mid-Ordovician impact structures. Although there are pre-Ordovician and early Ordovician rocks in the eastern third of Australia, these have been strongly tectonised, and were thus removed from consideration. The Australian continent straddled the equator during the period of interest, and the area of suitable crust is estimated at 1938,036 km^2.

North America. The North American Craton is well suited to preservation of Ordovician impact structures, and a considerable proportion of those recognised globally are situated there. The North American Cordillera along the west side of North America is an extensive belt of recently tectonised rock, and so was excluded from the area calculation. Laurentia also straddled the equator during the period of interest, and the area of suitable crust is estimated at 4578,367 km^2.

Europe. Most of Europe is poorly suited to preservation of Ordovician

impact craters, and yet this small region contains a large proportion of those recognised (Schmieder and Kring, 2020). Fig. 4 indicates that much of Scandinavia (western Baltica) is well suited despite recent glaciation, and all of the Ordovician impact structures in Europe are located in this region. Small areas in western France, Scotland and Czechia were deemed suitable and included in the area calculation. The recently tectonised regions in southern Europe are considered unsuitable. The region containing all of the Ordovician impact structures in Europe drifted from ~35–30°S to 30–15°S over the period 466 to 450 Ma, rotating anticlockwise. All of this region (1108,872 km^2) is included as proximal to the equator for the purposes of this calculation. A small area of interest in France (29,184 km^2) moved from ~ 50°S to 35°S over the period of interest and thus is considered distal to the equator.

Russia, including eastern Baltica. Fig. 4 shows that relatively small areas are well suited to preservation of Ordovician impact craters in Russia. To the east of Scandanavia, eastern Baltica is also well suited to crater preservation (and contains two Ordovician craters). Appropriately aged rocks in the Altaids have been deformed since the Ordovician and were excluded. Large areas of flat-lying Ordovician aged rocks north of Lake Baikal and surrounding the Siberian Traps (indicated in dark blue) were not included in the area calculation (because the GIS data do not distinguish between early, middle and late Ordovician), but they would be well suited to preservation of L chondrite meteorite and micrometeorite material. Over the period of interest, Siberia swept northward across the equator into low northern latitudes; all of this region and Baltica (1518,689 km^2) were thus proximal to the equator.

India. Much of the main continent of India, including Sri Lanka, is well suited to preservation of Ordovician impact craters. Northern India, Nepal and Bangladesh have been affected by the Himalayan collision and were excluded from the area calculation. During the period of interest, the southernmost part of the Indian Craton drifted from ~35°S to ~30°S, so all of this craton is included as the proximal to the equator, representing an area of 1171,670 km^2.
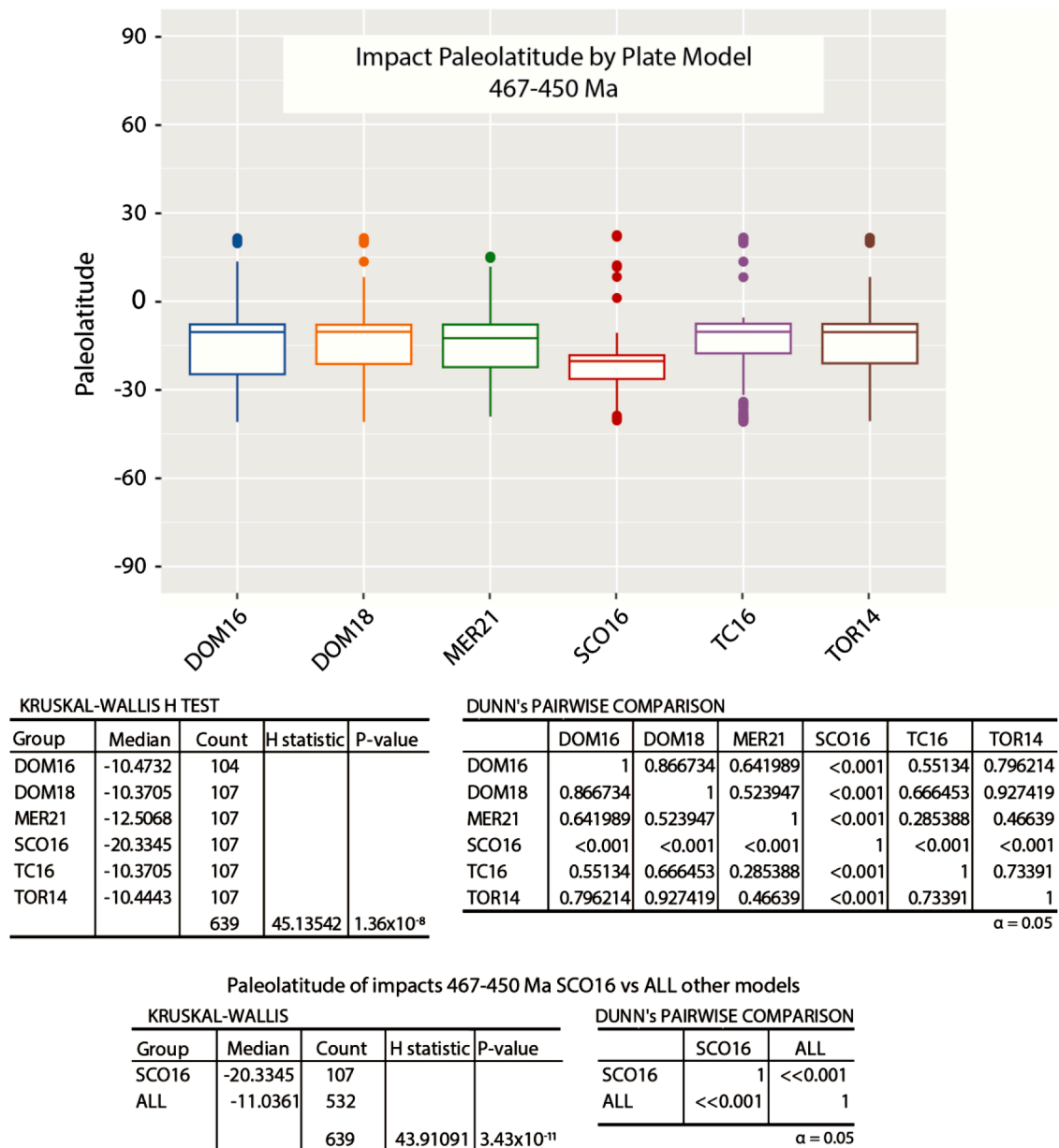
Fig. 3. Statistical comparison of the paleolatitude distribution of asteroid impacts 467–450 Ma grouped by plate model.

China. Fig. 4 shows that much of the pre-Ordovician crust in China has undergone recent tectonism. The North and South China Cratons experienced much Jurassic and Cretaceous magmatism and erosion has exposed these plutons, so we surmise that this would have removed all old impact craters, and indeed there is only one 50 k.y. old crater in China. The plate reconstructions show that China has been subject to extensive tectonism since the Ordovician, so there are no significant crustal elements suited to Ordovician impact structure preservation.

Africa. Much of the African continent consists of pre-Ordovician crust, albeit with considerable younger cover in broad areas. In terms of tectonic stability, Africa is well suited to preservation of Ordovician impact structures. The Ordovician aged rocks indicated in Fig. 5 were not included in the area calculation to be conservative. Most of Africa was situated south of 35°S from 466 to 450 Ma, although southern Africa was north of this latitude. The area of suitable crust situated south of 35°S is estimated at 24,875,914 km^2, and the area north of this latitude is 2193,000 km^2.

South America. Eastern South America consists of several stable ancient cratons well suited to preservation of Ordovician impact

structures. The Andes are not suitable for preservation of old impact structures. There are no impact craters recognised in South America that could plausibly be from the Ordovician impact spike. All of the suitable South American crust was distal to the equator from 466 to 450 Ma, and the area of suitable crust is estimated at 4821,352 km^2.

2.3. Multi-distance spatial cluster analysis (Ripley's K Function)

To evaluate the null hypothesis that the distribution of impacts is completely spatially random, multi-distance spatial cluster analysis (Ripley's K Function; Ripley, 1976) was conducted using ArcGIS. This approach evaluates the number of neighbouring features associated with each feature that are closer than the distance being evaluated, at multiple scales. This method illustrates how the spatial clustering or dispersion changes with various scales. If the data are completely spatially random, the multi-distance cluster analysis will yield a 1:1 correlation (expected K values) between the L(d) transformed Ripley's K function and the specified distance. Data that are clustered will lie above the 1:1 line and data that are dispersed will lie below the 1:1 line at
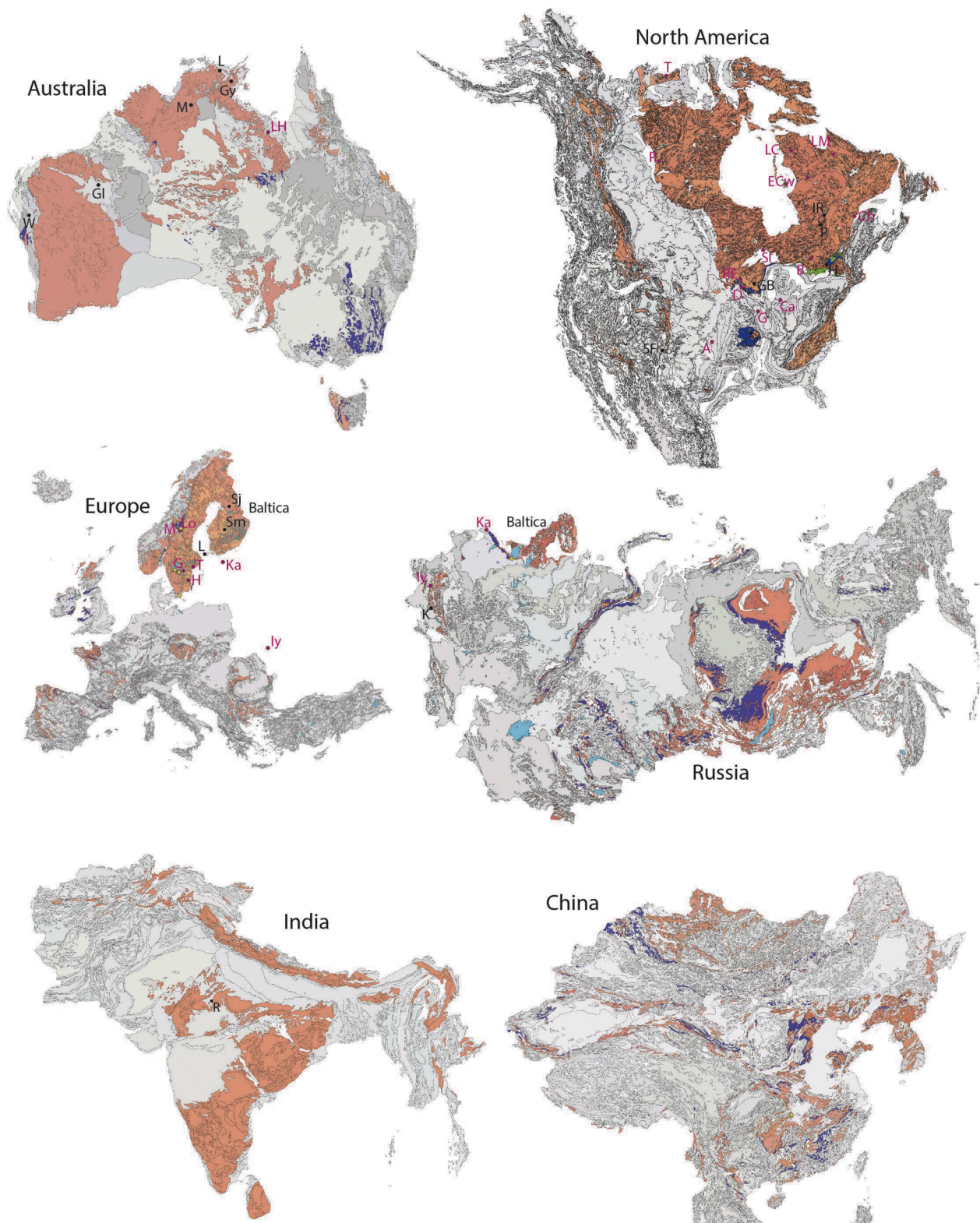
Fig. 4. Areas of continental crust proximal to the equator during the Ordovician. Areas older than Ordovician are indicated in salmon colour, Ordovician rocks are dark blue, and younger are grey. Light blue indicates lakes in Europe and Russia. The labelled pink points are the recognised Ordovician impact spike craters: in Australia, Lawn Hill (LH); in North America, Tunnunik (T), Pilot (P), Lac Couture (LC), East Clearwater Lake (ECw), La Moinerie (LM), Charlevoix (Ch), Brent (B), Slate Islands (SI), Rock Elm (RE), Decorah (D), Calvin (Ca), Glasford (G), Ames (A); in Europe, Lochne (Lo), Malingen (M), Granby (G), Tvaren (T), Hummeln (H), Ilyinets (Iy) and Kardla (Ka) (the latter two are situated on the western edge of the map for Russia). The labelled black points are impact structures with very poorly defined ages that could plausibly be Ordovician in age (Parisi et al., 2024; Schmieder and Kring, 2020), but have not been included in our considerations: Goyder (Gy), Glikson (Gl), Matt Wilson (M), Woodleigh (W), Liverpool (L), Glover Bluff (GB), Crooked Creek (CC), Santa Fe (SF), Holleford (H), Île Rouleau (IR), Presqu'île (P), Lumparn (L), Saarijärvi (Sj), Summanen (Sm), Kamenetsk (K), Ramgarh (R).
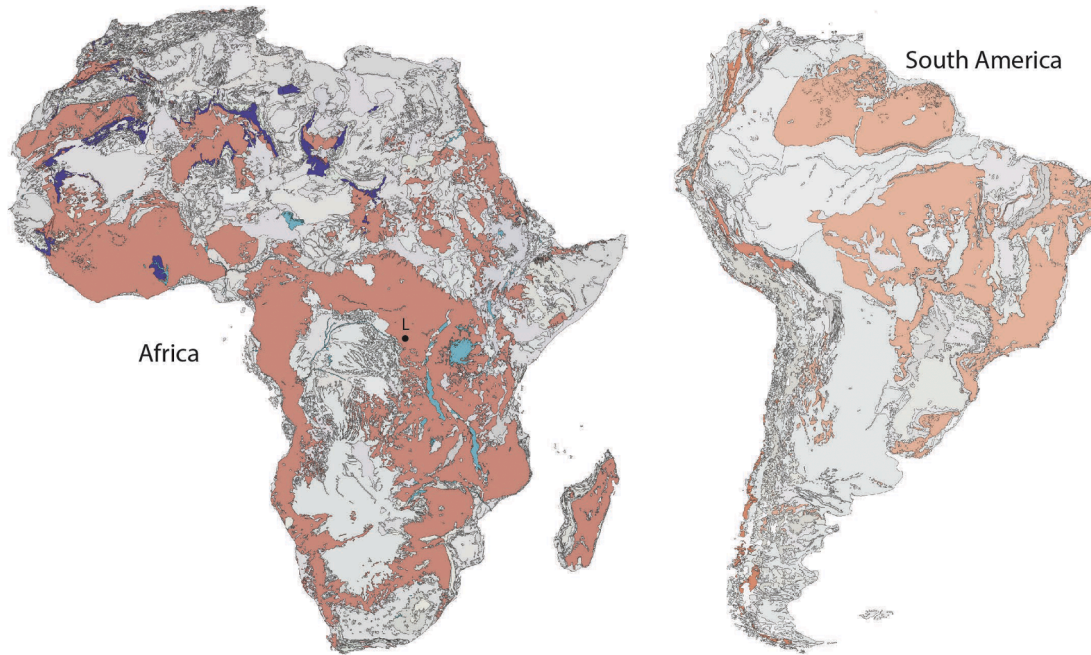
Fig. 5. Areas of continental crust distal to the equator during the Ordovician. Areas older than Ordovician are indicated in salmon colour, Ordovician rocks are dark blue, and younger are in grey. Light blue indicates lakes in Africa. The labelled point (L) in Africa is the Luizi impact structure, which has a very poorly defined age that could plausibly be Ordovician, constrained to be between 0 and 573 Ma (Schmieder and Kring, 2020).

varying distances (x-axis). When the observed K values are larger than the expected K value for a specific distance, the distribution is more clustered than a random distribution at that distance, and vice versa regarding dispersion. Distance is a calculation in-built in the statistical model and calculated as: maximum distance value is 25 % of the maximum length of a minimum enclosing rectangle around the impacts (increments = maximum distance/n iterations).

Multi-distance spatial cluster analysis revealed that for modern impact craters formed within the last 40 m.y., there is a small degree of statistically significant clustering of impacts at small distances (Fig. 6A). In distinct contrast, for Ordovician impacts (reconstructed at 460 Ma using MER21), there is a high degree of statistically significant clustering of the impacts at a wide range of distances (Fig. 6B). This substantiates our assertion that the distribution of Ordovician impacts is unlikely the result of random chance.

2.4. Simple estimate of the Roche Limits for Earth

A simple estimate of the approximate bounds on the range of Roche Limits for breakup of an L chondrite asteroid at Earth (radius = 6,371,000 m; avg density = 5513 kg m^{-3}) can be made by calculating the solid body Roche Limit using the density of L chondrites (3350 kg m^{-3}), and the liquid body Roche Limit (approximating a cohesionless rubble pile) using the measured density of Itokawa (1900 kg m^{-3}), which is thought to be comprised of low metal ordinary chondrite material (Fujiwara et al., 2006).
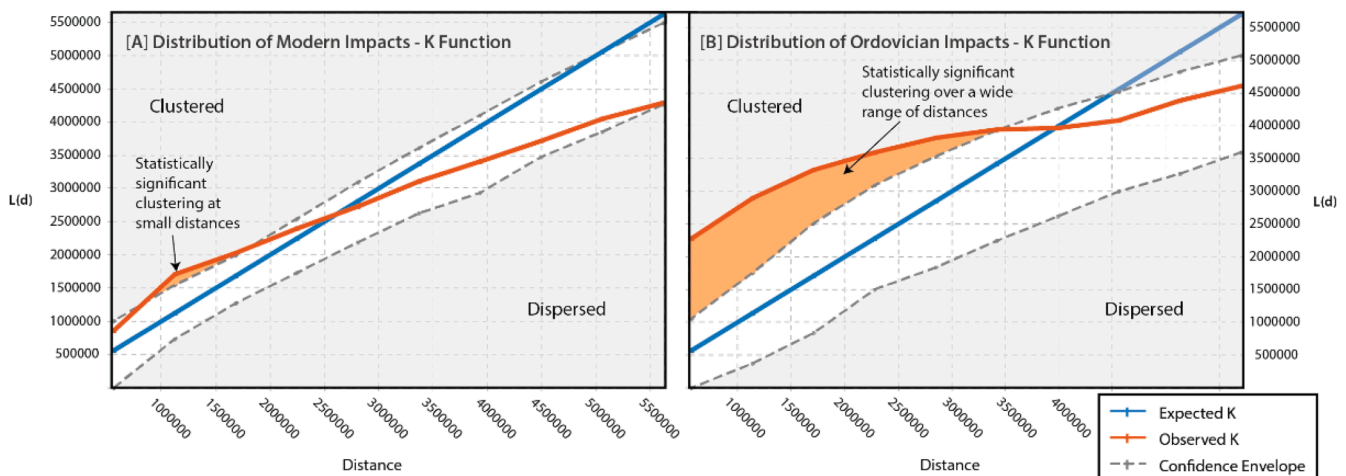
For the solid body Roche Limit:

Fig. 6. Statistical comparison of impact clustering for the last 40 m.y. using current geography (A) and the Ordovician craters at 460 Ma using MER21 (B). The blue line (with white confidence envelope) shows the expected distance between randomly distributed craters (expected K) based on the data, and the orange line shows the observed distance (observed K). When the observed distance is larger than the expected distance for a particular distance, the distribution is more clustered than a random distribution at that distance. Shaded orange areas show distances that fall outside the confidence envelope and are statistically significantly clustered. L(d): modified Ripley's K function. Distance: modelled distance.

$$d_s \approx R_E \left(2 \frac{\rho_E}{\rho_A} \right)^{1/3} \qquad (1)$$

In which case, $d_s \approx 3106$ km above the Earth's surface. Here, d_s is the solid body Roche Limit, R_E is Earth's radius, ρ_E is Earth's density, and ρ_A is the asteroid's density. And, for the liquid body Roche Limit (d_l):

$$d_l \approx 2.44 R_E \left(\frac{\rho_E}{\rho_A} \right)^{1/3} \qquad (2)$$

In which case, $d_l \approx 15{,}801$ km above the Earth's surface.

3. Discussion

3.1. Paleolatitudes of Ordovician impact craters

Fig. 7 shows the continental plate and impact crater positions from 467 to 450 Ma (Middle Ordovician) for the most recent global paleogeographic reconstruction model (Merdith et al., 2021). Although there are large errors on the age estimates of some craters (Figs. 1 and 2), this period captures the relevant crater positions before the southernmost continents became ice covered (Scotese, 2021). In the six plate reconstruction models we evaluated, the impact craters are all distributed relatively close to the equator (Figs. 2, 3, 7), primarily $\leq 30° \pm 13.4°$ ranging as far as $39°S$ at maximum possible distance from the paleo-equator in the most recent model of (Merdith et al., 2021).

It is notoriously difficult to ascertain the composition of bolides that created impact structures. Lockne crater was likely formed by an L chondrite impactor, Clearwater East possibly formed by an L or H chondrite impactor, and the bolide composition is either unknown or masked by considerable uncertainty for the other 19 craters of interest (Schmitz et al., 2022).

There are 17 additional craters that have very poorly defined ages that could plausibly be Ordovician in age (Schmieder and Kring, 2020); of these, only Luizi would be positioned at high latitude (Figs. 4 and 5). Lawn Hill crater in Australia has an age close to the beginning of the period of interest (472 $\pm$ 8 Ma) (Darlington et al., 2016). It and/or several others of comparable age (Fig. 1) may have formed during the suggested near-Earth asteroid break-up event (see below). The paleogeographic reconstruction models hint that the oldest impact structures have greater variation in paleolatitude than the younger craters (Fig. 2).

3.2. Probability that the crater distribution is random

For impact craters from the period of interest to be observed today, they need to have impacted older continental crust that subsequently avoided significant reworking and/or erosion. The average global temperature at the beginning of the period of interest (ca. 466 Ma) was warm enough that there was likely no ice cap at the South Pole, but rapid cooling from then is thought to have generated an ice sheet reaching low latitudes (~30°) from about 450 to 444 Ma (Scotese, 2021). Thus, in all plate reconstruction models, the components of Africa and South America are well suited to preservation of impact craters from 466 to 450 Ma, but the intensity of global cooling was such that ice sheets may have inhibited preservation of impact craters from 450 to 444 Ma. The brief Late Ordovician glaciation is considered unlikely to have removed evidence of impact structures because the majority of the craters of interest are well preserved despite being affected by recent continental glaciation in North America and Europe. Of the craters of interest, 14 have ages with probability ≥ 0.5 of occurring within the 466 to 450 Ma window. The differences between the plate models impart only minor variations in our estimates of the area of crust that could preserve Ordovician impact craters as a function of latitude.

The probability calculation is based on the proportion of appropriate crustal surface area within a $\pm 30°$ paleolatitude band for the MER21
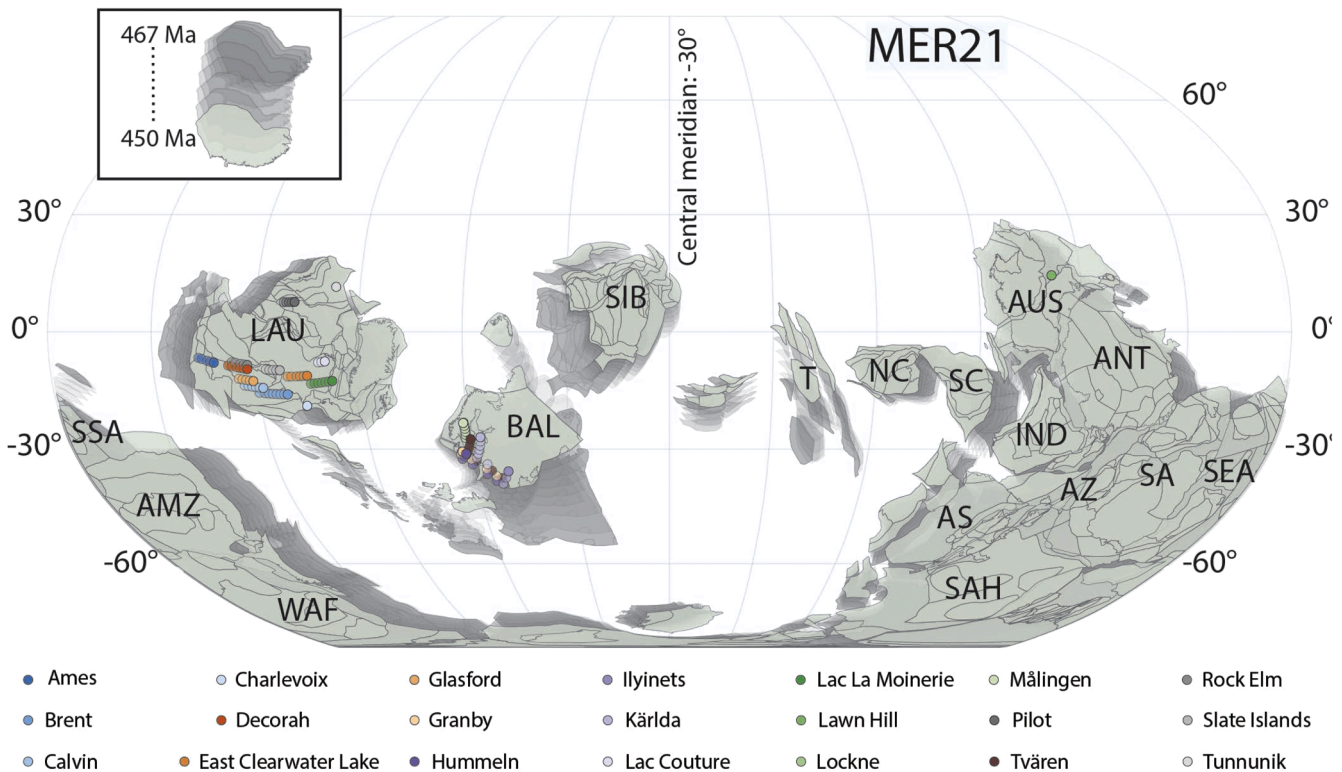

Fig. 7. Positions of the Ordovician impact craters on the reconstructed plate positions of the MER21 model, showing the movement of continents and trace of impact sites from 467 to 450 Ma. AMZ, Amazonia; ANT, Antarctica; AS, Arabian Shield; AUS, Australia; AZ, Azania; BAL, Baltica; IND, India; LAU, Laurentia; NC, North China; SA, Southern Africa; SAH, Saharah; SC, South China; SEA, South-eastern South America; SIB, Siberia; SSA, Southern South America; T, Tarim; WAF, West Africa.

model for 466 to 450 Ma, compared to that at higher latitudes. The underlying principle here is that typical impacts are distributed randomly across the globe, whereas impacts resulting from a body that broke up during a close encounter would fall in a latitudinal band.

In total, the area of continental crust considered suitable of preserving Ordovician impact structures proximal to the paleo-equator ($\pm 30°$) based on MER21 is 12,508,635 km^2. The suitable area of crust distal to the paleo-equator is 29,697,266 km^2. Thus, the proportion of proximal crust is estimated at 29.6 %. So, for the MER21 model, the probability that each impact would randomly occur in the proximal region rather than the distal region is 0.296, and this probability is multiplied through the number of impact events. Fourteen craters have age ranges that >50 % overlap the 466 and 450 Ma period (all 21 craters have age ranges that overlap this period to some extent; Fig. 1). The binomial probability that at least 14 impacts occurred in crust proximal to the equator due to random impacts is 3.96×10^{-8} (or about 1 in 25 million):

$$P(X) = \binom{n}{X} \cdot p^X \cdot (1-p)^{n-X} \tag{3}$$

where, $\binom{n}{X} = \frac{n!}{X!(n-X)!}$, p = probability of a single success = 0.296, n = number of trials = 14, and X = number of successes = 14.

If additional impacts are identified in the proximal range during the impact spike period, these would further reduce the probability (e.g., probability of 20 successes = 2.67×10^{-11}). Notably, as normal random impact events likely occurred during the Ordovician impact spike (i.e. impacts could be outside of the equatorial band) the binomial probability is not significantly reduced by one or two fewer successes. For example, if two impacts are later considered to have formed through unrelated impact events, the binomial probability for 12 random impacts successfully occurring in proximal crust is 2.04×10^{-5}. The situation for DOM18 is essentially the same.

The multi-distance spatial cluster analysis independently confirms that the crater distribution is non-random, showing that the Ordovician impacts have a high degree of statistically significant clustering at a wide range of distances. By comparison, impact structures formed in the last 40 m.y. are unclustered, consistent with the normal randomly distributed cratering of the Earth (cf. Rumpf et al., 2016).

3.3. Formation of a debris ring may explain the non-random crater distribution

It has long been known that chains of impact craters form in response to single bodies breaking up as they near a planet or moon. A latitudinal band of impacts formed in Jupiter's atmosphere, for example, after comet Shoemaker-Levy 9 broke up around the planet (Zahnle and MacLow, 1994). But these linear bands of craters form in geologically short timeframes: Shoemaker-Levy 9 was initially captured by Jupiter, then after 20–30 years of orbits broke up in July 1992, before the many impactors collided between July 16 and 22, 1994. We have demonstrated that it is highly improbable that the non-random, latitudinal and quasi-equatorial band of Ordovician impact craters were produced by many different bodies derived from separate locations in the inner Solar System. The observation that sedimentary rocks from this time are two to three orders of magnitude more enriched in meteorite debris and 99 % of this is from the L chondrite parent body (Terfelt and Schmitz, 2021) also strongly suggests that a single body was involved. We suggest the most appropriate explanation is that the meteorite debris in the sedimentary rocks and the impactors came from a large LCPB fragment that was tidally disrupted during a close encounter with the Earth at 466 Ma. However, unlike the Shoemaker-Levy 9 event, and other crater chain forming events, the enhanced L chondrite sedimentation and impact cratering appear to have persisted for up to 40 m.y. (noting that the duration of this period is currently poorly constrained). To explain these observations, we suggest that fragments of disrupted LCPB were

captured by the Earth, forming a debris ring that gradually decayed to explain both the equatorial distribution of impact craters, and the exponential decrease in meteorite debris in the sedimentary rocks. Rings around other planets are known to persist considerably longer than this; Saturn's rings are thought to be on the order of 100–400 m.y. old (Kempf et al., 2023).

For a small body to be captured by a planetary body it must enter that planet's Hill Sphere (region of gravitational dominance), and be slowed down to below its escape velocity (Araujo et al., 2008). All Solar System planets readily capture asteroids (Bailey, 1972), and there is a constant population of temporarily captured objects around the Earth (Granvik et al., 2012) where km-scale asteroids are captured about once every 10 m.y. (Fedorets et al., 2017). In a process that occurs much more rarely, particularly around smaller planets, small bodies break up when they pass within a planet's Roche Limit, the distance within which objects are pulled apart by tidal forces (Williams, 2003). Because the gravitational forces involved in capture are stronger within Earth's Roche limit than at larger distances within the Hill sphere, capture is more likely when a body passes through the Roche limit (cf. Hyodo et al., 2017). Fragment orbits that are initially elliptical become circularised over time in response to collisional interaction, producing a ring inside the Roche limit (Charnoz et al., 2018). Planetary rings are refined as perpendicular motions of these fragments are minimised relative to their motions in the equatorial plane, which occurs because planets bulge at their equators creating a gravitationally-controlled preferred orbital plane (Tiscareno and Hedman, 2014). Thus, material deorbiting onto a planet from a ring is preferentially distributed close to the equator.

The Roche Limit for a solid L chondrite body (bulk density 3350 kg m^{-3} (Britt and Consolmagno, 2003) is 3106 km above the Earth's surface (9477 km from the center), whereas that for a rubble-pile asteroid is far greater. For S-class rubble pile asteroid Itokawa it would be ~15,800 km above the surface (22,171 km from the center; density from (Fujiwara et al., 2006) and assuming cohesionless rubble; a precise value cannot be calculated without knowing the asteroid shape and internal cohesion properties). Within this transition zone between the rubble pile and the solid body Roche Limit, a body consisting of a power law collection of fragments (as expected for a rubble pile (Sánchez and Scheeres, 2014) would break up and disperse, with abundant miniscule fragments forming a ring, and the largest solid fragments forming moonlets (see also Hyodo et al., 2017). Another possibility is a solid body heavily fractured by impacts, which would also break up within this transition zone, probably forming a higher proportion of larger fragments than in the rubble pile body. Given that longevity of the L chondrite event (ca. 40 Ma), break-up of a power law rubble pile asteroid, or a heavily impact-fractured body, is our preferred model. Thus, there was probably a debris ring around the Earth from about 466 Ma that gradually dissipated over an extended time period. The lack of increased meteorite flux associated with other known asteroid break-up events (Terfelt and Schmitz, 2021) also implies that a close break-up event is a better explanation for the Ordovician impact spike. And, the small size of the orbital window that such a body would need to pass through to break up in this way means that such events are very rare; this is consistent with the extraterrestrial chromite data, which suggest that this has happened only once in the last 540 m.y. and probably longer (Martin et al., 2018; Schmitz et al., 2022).

Much of the Roche Limit transition zone is within the current Earth's exosphere, extending from 700 to 10,000 km. Objects passing through a comparable tenuous outer edge of the atmosphere in the Ordovician would be slowed through friction, resulting in orbital decay and collision with the Earth. Interactions between the exosphere and ring material would tend to remove gases by chemical reaction with ring particles, reducing friction and slowing down decay of the ring. However, tidal decay would also play an important role in this setting. Given that the outermost Roche Limit (15,800 km above the surface) is well within the geostationary orbit position (35,786 km above the equator), much of the debris would undergo tidal decay and deorbit to the Earth's

surface (see Rosenblatt et al., 2016). Tidal decay affects larger bodies more than small, so larger fragments will tend to sweep up smaller fragments and grow in the process, but this can only apply outside the Roche Limit. Thus, larger debris fragments that, after the initial break-up event, are positioned outside the Roche Limit and inside geosynchronous orbit would tend to grow as they migrate inward, and then break up again upon reaching the Roche Limit. This process would gradually clear out the ring. Models applied to the evolution of a giant impact-derived debris disk around Mars suggest that this process may have formed Phobos and Deimos, these having grown from outward migrating material from above Mars-synchronous orbit, with material inside orbit falling back to the Martian surface (Rosenblatt et al., 2016).

Capture of an L chondrite body from the asteroid belt would begin with an elliptical orbit, breakup of that body at a perigee inside ~15,800 km, with some of the resulting fragments interacting with the exosphere as their orbits became circularised and migrated to the equatorial plane, and higher altitude fragments undergoing tidal decay. Fragments outside geosynchronous orbit might be expected to dissipate through collisional interactions and the Yarkovsky effect (Vokrouhlický et al., 2000), or perhaps form one or more mini-moons through tidal dissipation (cf. Rosenblatt et al., 2016) that are no longer with us.

Argon dating of L chondrite meteorites has found that many have ages indicating a major shock event at ~470 ± 6 Ma, and this age has been linked to the L chondrite asteroid break-up event purported to have scattered fragments throughout the inner solar system (Korochantseva et al., 2007). It is possible that a major collisional event in the asteroid belt did occur (explaining the Ar data), sending a single large L chondrite fragment into a Jupiter-resonant orbit and from there onto an Earth-encountering orbit. This process is the main mechanism (along with Yarkovsky and YORP effects) that continuously sends asteroid fragments < 30 km from the asteroid belt onto planet-encountering orbits (Bottke et al., 2015). This would explain why 99 % of the meteorite debris in sediments on Earth is L chondrite material (Schmitz et al., 2019), rather than contributions from two bodies colliding (one sample of another meteorite type has been found; Schmitz et al., 2016). Note that our model does not require a collision in the asteroid belt, but a collision at ~470 Ma may be part of the history.

A recent analysis of impact craters on Earth, Mars and the Moon recognised the Ordovician impact spike on Earth, but found no equivalent on Mars or the Moon (Lagain et al., 2022). These authors then suggested that there was no anomalous impact cratering rate during the Ordovician on the basis that: (1) the lack of anomalous cratering on Mars and the Moon is inconsistent with breakup of the L chondrite parent body causing a shower of debris through the inner solar system, and (2) a preservation bias favoured crater preservation in the Ordovician causing an apparent spike in cratering rate (having recognised the equatorial distribution). However, the first point actually supports our hypothesis in that it is consistent with break-up of a single body proximal to Earth rather than break-up of an LCPB in the asteroid belt; the latter would be expected to affect Mars more than Earth. Secondly, regarding the preservation bias argument, Legain et al. (2022) considered only 10 of the possible 21 Ordovician impact craters, noting that three of these formed in shallow seas, and six impacted into sedimentary rocks. However, of the 21 Ordovician craters, 5 were into crystalline targets (23.8 %), and 10 into mixed crystalline and sedimentary targets (47.6 %), and only 6 into sedimentary targets (28.6 %; data in (Osinski et al., 2022; Schmieder and Kring, 2020). Thus, the proportion of Ordovician impacts into crystalline, mixed and sedimentary targets are similar to Earth's entire impact crater record, with slightly more impacts into mixed targets and less impacts into sedimentary and crystalline targets (all Earth structures: crystalline = 29 %, mixed = 30 %, sedimentary = 40 %; Osinski et al., 2022). Furthermore, the logic about sediments near the equator preferentially preserving craters relative to sediments at higher latitudes is flawed: for example, the area of minimally disturbed Ordovician sedimentary rocks through the high-paleolatitude Sahara region (Ghienne et al., 2023) is far larger than

the area of comparable rocks in Europe and North America (compare Figs. 5 and 7). And arguably, preservation of impact structures in actively accumulating sedimentary systems is less favourable than for craters impacting solid rock on land because tides, currents, wave action and new sedimentation combine to rapidly destroy and bury evidence of loosely consolidated, topographically irregular geological features at the surface. Indeed, amongst Earth's entire record of 201 craters, only 13 (6.5 %) may have been partially preserved in sediments that were unconsolidated at the time (Osinski et al., 2022). However, 24 % of the Ordovician craters appear to have been partially preserved by unconsolidated sediments, which may have been caused by the higher sea levels and greater extent of continental shelf before the global cooling towards the end of the Ordovician. We acknowledge that ancient impacts preserved by disruption of sedimentary strata are arguably easier to recognise than those affecting crystalline targets. Lastly, the evidence for increased flux of material to Earth in the Ordovician is not just from the cratering rate; the large increase in L chondrite debris in sedimentary rocks away from craters is well-established (Schmitz et al., 2022), and a significant increase in the abundance of seismic- and tsunami-related megabreccia deposits is also recorded at this time, implying increased impact activity (Parnell, 2009).

Break-up of a single body proximal to Earth would also explain the extremely short cosmic ray exposure (CRE) ages of L chondrite debris from Thorsburg quarry, which indicate that the material broke up < 100 k.y. before being deposited, and the observed increase in CRE ages from the base to the top of the sequence (from 0.1 to 1.2 Ma) (Heck et al., 2004, 2008). By comparison, stony meteorites typically have CRE ages ranging up to 100 Ma, with most ordinary chondrite meteorites having ages in the ranges 5–30 Ma (H chondrites), 5–50 Ma (L chondrites), and 5–60 Ma (LL chondrites), indicating the normal timescale of their transfer from the asteroid belt to the Earth (Herzog and Caffee, 2014).

3.4. Future tests of the hypothesis

There is a clear need to determine whether L chondrite impactors formed the Ordovician craters in the period of interest. The longevity of the ring (or period of enhanced extraterrestrial flux) is also poorly constrained and needs to be refined by a combination of higher resolution extraterrestrial chromite counting from sedimentary rocks younger than 466 Ma, and chromite CRE ages. The latter may provide insights into progressive break-up of larger bodies within the ring system. It is plausible that the apparent bimodality in the crater ages (Fig. 1) reflects a system where a small moon formed from the initial debris that found itself between 15,800 km and 35,786 km altitude (above Roche limit, below geostationary orbit) and then broke up again as tidal decay brought the body down through the Roche Limit (perhaps at ~455 Ma) (Hesselbrock and Minton, 2017; Rosenblatt et al., 2016). This could be tested by refined crater dating, and discovery of an additional spike in meteorite debris in ~455 Ma sediments would also support such a hypothesis. Mathematical modelling of ring evolution, as exemplified by Rosenblatt et al. (2016), needs to be undertaken to test this concept and provide insights into ring longevity.

If a ring system existed, accretion of its material to Earth would add more meteoritic debris to sediments formed near the equator (Rosenblatt et al., 2016), so we predict a systematic decrease in abundance of L chondrite material in appropriately aged sedimentary rocks with increasing distance from the paleo-equator (normalised to sediment accumulation rate). Although difficult to determine, tsunami-related megabreccia deposits might be expected to reflect a more intense tsunami waves closer to the equator. Impactors deorbiting from a debris ring would be expected to transit the atmosphere slowly by comparison with all other impactors, and likely impact at shallow angles (Schultz and Lutz-Garihan, 1982). Evidence of shallow impact angle is primarily preserved in ejecta aprons and although preservation of such ancient aprons would be extremely rare due Earth's to rapid erosion rates (Pierazzo and Melosh, 2000), this is something to be tested if

possible.

Gravitational dynamics modelling could test the plausible limits of the initial ring formation process. For use in this modelling, an estimate for the size of the L chondrite asteroid can be derived from the size of the bodies needed to form the observed craters (derived from Marcus et al., 2024), an estimate of the number of caters not preserved, the amount of L chondrite debris preserved in sedimentary rocks and assuming end-member densities for the body. A source of uncertainty is the preservation rate for the Ordovician. Using the average slope of the frequency density distribution function from figure 12b in Kenkmann (2021), the Ordovician impact and preservation rate compared to today is roughly approximated at 0.1; close to our estimate for the fraction of crust suitable for preserving Ordovician impact craters relative to the land area today (0.084), so we consider using the latter to be a reasonable approach. We thereby estimate that the body may have been on the order of 12.5 km diameter for a rubble pile, or 10.5 km diameter for a solid body (Supplementary Material). These are underestimates because an unconstrained amount of L chondrite material would be ejected from Earth's orbit during break-up and disk evolution.

3.5. Speculations on the implications for paleoclimate

If an equatorial ring existed, the axial tilt of the Earth relative to the Sun would cause it to shade the winter hemispheres of the Earth, and reflected sunlight would slightly increase the solar flux to the summer hemispheres. This would accentuate winter cooling (Pearson et al., 2006) and slightly increase summer heating, increasing the temperature range experienced through the seasonal cycle, but decreasing the temperature gradient between equator and pole in the winter hemisphere (Fawcett and Boslough, 2002). Dust in the atmosphere produced by impacts would also contribute to cooling. We suggest that this global cooling mechanism might explain the dramatic plunge into global icehouse conditions that developed over 463–444 Ma (Rasmussen et al., 2016; Scotese, 2021), perhaps solving the puzzle of why such intense cooling happened despite high atmospheric CO_2 (Lenton et al., 2012). A rapid-onset increase in temperature variability would create the need for adaptation in living organisms, potentially providing an explanation for the Great Ordovician Biodiversification Event. We suggest that the ~8 °C of global cooling for this period (Scotese, 2021) could be used to calculate how much of the Sun's energy was blocked by the ring, and therefore how diffuse the ring was (cf. Fawcett and Boslough, 2002). Furthermore, dissipation of a ring would cease the cooling effect and cause global warming back to typical global temperatures, and we suggest that this might explain the rapid warming from 444 to 437 Ma (Scotese, 2021) (Fig. 1). The average global temperature curve of Fig. 1 might thereby date the duration of the ring (which would be ~22 m.y.) and this could be tested through climate modelling.

4. Summary and conclusions

We have suggested that a large L chondrite asteroid had a near miss encounter with Earth at ca. 466 Ma, which caused it to break up as it passed through Earth's Roche limit. This can explain why sedimentary rocks from this time contain 99 % L chondrite material at abundances 2–3 orders of magnitude above background, with extremely brief CRE ages. We have further suggested that the resulting fragments formed a debris ring that decayed over several tens of millions of years resulting in an anomalous spike in impact cratering rate. This hypothesis may explain why all impact structures from this time are located proximal to the equator; impacts from bodies originating in the asteroid belt are expected to be randomly distributed across the globe. We have estimated the probability that this impact structure distribution resulted from random unrelated impactors at 1 in 25 million. We speculate that this ring may have promoted the coldest global cooling event in the last 540 million years, the Hirnantian Icehouse period.

References

Alvarez, L.W., Alvarez, W., Asaro, F., Michel, H.V., 1980. Extraterrestrial cause for the cretaceous-tertiary extinction. Science 208, 1095–1108.

Araujo, R.A.N., Winter, O.C., Prado, A.F.B.A., Vieira Martins, R., 2008. Sphere of influence and gravitational capture radius: a dynamical approach. Mon Not R Astron Soc 391, 675–684.

Bailey, J., 1972. Studies on planetary satellites. Satellite capture in the three-body elliptical problem. Astronom J 77, 177–182.

Bottke, W.F., Brož, M., O'Brien, D.P., Bagatin, A.C., Morbidelli, A., Marchi, S., 2015. The Collisional Evolution of the Main Asteroid Belt., in: Michel, P., DeMao, F.E., Bottke, W.F. (Eds.), Asteroids IV Univ. of Arizona, Tucson, pp. 701–724.

Britt, D.T., Consolmagno, G.J.S.J., 2003. Stony meteorite porosities and densities: a review of the data through 2001. Meteorit Planet Sci 38, 1161–1180.

Charnoz, S., Canup, R.M., Crida, A., Dones, L., 2018. The origin of planetary ring systems. In: Tiscareno, M.S., Murray, C.D. (Eds.), Planetary ring systems: properties, structure, and evolution. Cambridge University Press, pp. 517–538.

Darlington, V., Blenkinsop, T., Dirks, P., Salisbury, J., Tomkins, A.G., 2016. The Lawn Hill annulus: an Ordovician meteorite impact into water-saturated dolomite. Meteorit Planet Sci 51, 2416–2440.

Domeier, M., 2016. A plate tectonic scenario for the Iapetus and Rheic oceans. Gondw Res 36, 275–295.

Domeier, M., 2018. Early Paleozoic tectonics of Asia: towards a full-plate model. Geosci Front 9, 789–862.

Fawcett, P.J., Boslough, M.B.E., 2002. Climatic effects of an impact-induced equatorial debris ring. J Geophys Res 107, No. D15, 4231.

Fedorets, G., Granvik, M., Jedicke, R., 2017. Orbit and size distributions for asteroids temporarily captured by the Earth-Moon system. Icarus 285, 83–94.

Fujiwara, A., Kawaguchi, J., Yeomans, D.K., Abe, M., Mukai, T., Okada, T., Saito, J., Yano, H., Yoshikawa, M., Scheeres, D.J., Barnouin-Jha, O., Cheng, A.F., Demura, H., Gaskell, R.W., Hirata, N., Ikeda, H., Kominato, T., Miyamoto, H., Nakamura, A.M., Nakamura, R., Sasaki, S., Uesugi, K., 2006. The rubble-pile asteroid Itokawa as observed by Hayabusa. Science 312, 1330–1334.

Ghienne, J.-F., Abdallah, H., Deschamps, R., Guiraud, M., Gutiérrez-Marco, J.C., Konaté, M., Meinhold, G., Moussa, R., Rubino, J.-L., 2023. The Ordovician record of North and West Africa: unravelling sea-level variations, Gondwana tectonics, and the glacial impact. In: Servais, T., Harper, D.A.T., Lefebvre, B., Percival, I.G. (Eds.), A Global Synthesis of the Ordovician System: Part 2, pp. 199–252.

Granvik, M., Vaubaillon, J., Jedicke, R., 2012. The population of natural Earth satellites. Icarus 218, 262–277.

Heck, P.R., Schmitz, B., Baur, H., Halliday, A.N., Wieler, R., 2004. Fast delivery of meteorites to Earth after a major asteroid collision. Nature 430, 323–325.

Heck, P.R., Schmitz, B., Baur, H., Wieler, R., 2008. Noble gases in fossil micrometeorites and meteorites from 470 Myr old sediments from southern Sweden, and new evidence for the L-chondrite parent body breakup event. Meteorit Planet Sci 43, 517–528.

Herzog, G.F., Caffee, M.W., 2014. Cosmic-ray exposure ages of meteorites. In: Davis, A. M. (Ed.), Meteorites and Cosmochemical Processes. Elsevier, pp. 419–453.

Hesselbrock, A.J., Minton, D.A., 2017. An ongoing satellite–ring cycle of Mars and the origins of Phobos and Deimos. Nat Geosci 10, 266–269.

Hildebrand, A.R., Penfield, G.T., Kring, D.A., Pilkington, M., Camargo, Z., Jacobsen A., S. B., Boynton, W.V., 1991. Chicxulub Crater: a possible Cretaceous/Tertiary boundary impact crater on the Yucatán Peninsula. Mexico Geol 19, 867–871.

Hyodo, R., Charnoz, S., Ohtsuki, K., Genda, H., 2017. Ring formation around giant planets by tidal disruption of a single passing large Kuiper belt object. Icarus 282, 195–213.

Kempf, S., Altobelli, N., Schmidt, J., Cuzzi, J.N., Estrada, P.R., Srama, R., 2023. Micrometeoroid infall onto Saturn's rings constrains their age to no more than a few hundred million years. Sci Avanc 9, eadf8537.

Kenkmann, T., 2021. The terrestrial impact crater record: a statistical analysis of morphologies, structures, ages, lithologies, and more. Meteorit Planet Sci 56, 1024–1070.

Korochantseva, E.V., Trieloff, M., Lorenz, C.A., Buykin, A.I., Ivanova, M.A., Schwarz, W. H., Hopp, J., Jessberger, E.K., 2007. L-chondrite asteroid breakup tied to Ordovician meteorite shower by multiple isochron 40Ar-39Ar dating. Meteorit Planet Sci 42, 113–130.

Kring, D., Boynton, W., 1992. Petrogenesis of an augite-bearing melt rock in the Chicxulub structure and its relationship to K/T impact spherules in Haiti. Nature 358, 141–144.

Lagain, A., Kreslavsky, M., Baratoux, D., Liu, Y., Devillepoix, H., Bland, P., Benedix, G.K., Doucete, L.S., Servis, K., 2022. Has the impact flux of small and large asteroids varied through time on Mars, the Earth and the Moon? Earth Planet Sci Lett 579, 117362.

Lenton, T.M., Crouch, M., Johnson, M., Pires, N., Dolan, L., 2012. First plants cooled the Ordovician. Nat Geosci 5, 86–89.

Liao, S., Huyskens, M.H., Yin, Q.Z., Schmitz, B., 2020. Absolute dating of the L-chondrite parent body breakup with high-precision U-Pb zircon geochronology from Ordovician limestone. Earth Planet Sci Lett 547, 116442.

Marcus, R., Melosh, H.J., Collins, G., 2024. https://www.purdue.edu/impactearth/.

Martin, E., Schmitz, B., Schonlaub, H.-P., 2018. From the mid-Ordovician into the Late Silurian: changes in the meteorite flux after the L-chondrite parent breakup. Meteorit Planet Sci 53, 2541–2557.

Meinhold, G., Arslan, A., Lehnert, O., Stampfli, G.M., 2011. Global mass wasting during the Middle Ordovician: meteoritic trigger or plate-tectonic environment? Gondw Res 19, 535–541.

Merdith, A.S., Williams, S.E., Collins, A.S., Tetley, M.G., Mulder, J.A., Blades, M.L., Young, A., Armistead, S.E., Cannon, J., Sabin Zahirovic, S., Müller, R.D., 2021. Extending full-plate tectonic models into deep time: linking the Neoproterozoic and the Phanerozoic. Earth-Sci Rev 214, 103477.

Müller, R.D., Cannon, J., Qin, X., Watson, R.J., Gurnis, M., Williams, S., Pfaffelmoser, T., Seton, M., Russell, S.H.J., S, Z., 2018. GPlates: building a virtual Earth through deep time. Geochem Geophys Geosyst 19, 2243–2261.

Osinski, G.R., Grieve, R.A.F., Ferrière, L., Losiak, A., Pickersgill, A.E., Cavosie, A.J., Hibbard, S.M., Hill, P.J.A., Bermudez J, J., Marion, C.L., Newman, J.D., Simpson, S. L., 2022. Impact Earth: a review of the terrestrial impact record. Earth-Sci Rev 232, 104112.

Parisi, A.F., Catlos, E.J., Brookfield, M.E., Schmitt, A.K., Stöckli, D.F., Miggins, D.P., Campos, D.S., 2024. The Ordovician meteorite event in North America: age of the Slate Islands impact structure, northern Lake Superior, Ontario, Canada. Meteorit Planet Sci. https://doi.org/10.1111/maps.14183.

Parnell, J., 2009. Global mass wasting at continental margins during Ordovician high meteorite influx. Nat Geosci 2, 57–61.

Pearson, J., Oldson, J., Levin, E., 2006. Earth rings for planetary environment control. Acta Astronaut 58, 44–57.

Pierazzo, E., Melosh, H.J., 2000. Understanding oblique impacts from experiments, observations and modeling. Annu Rev Earth Planet Sci 28, 141–167.

Rasmussen, C.M., Ullmann, C.V., Jakobsen, K.G., Lindskog, A., Hansen, J., Hansen, T., Eriksson, M.E., Dronov, A., Frei, R., Korte, C., Nielsen, A.T., Harper, D.A.T., 2016. Onset of main Phanerozoic marine radiation sparked by emerging Mid Ordovician icehouse. Sci Rep 6, 18884.

Ripley, B.D., 1976. The second-order analysis of stationary point processes. J Appl Probab 13, 255–266.

Rosenblatt, P., Charnoz, S., Dunseath, K., Terao-Dunseath, M., Trinh, A., Hyodo, R., Genda, H., Toupin, S., 2016. Accretion of Phobos and Deimos in an extended debris disc stirred by transient moons. Nat Geosci 9, 581–583.

Rumpf, C., Lewis, H.G., Atkinson, P.M., 2016. The global impact distribution of Near-Earth objects. Icarus 265, 209–217.

Sánchez, P., Scheeres, D.J., 2014. The strength of regolith and rubble pile asteroids. Meteorit Planet Sci 49, 788–811.

Schmieder, M., Kring, D.A., 2020. Earth's impact events through geologic time: A list of recommended ages for terrestrial impact structures and deposits. Astrobiology 20, 91–141.

Schmitz, B., Farley, K.A., Goderis, S., Heck, P.R., Bergstrom, S.M., Boschi, S., Claeys, P., Debaille, V., Dronov, A., van Ginneken, M., Harper, D.A.T., Iqbal, F., Friberg, J., Liao, S., Martin, E., Meier, M.M.M., Peucker-Ehrenbrink, B., Soens, B., Wieler, R., Terfelt, F., 2019. An extraterrestrial trigger for the mid-Ordovician ice age: dust from the breakup of the L-chondrite parent body. Sci Adv 5, eaax4184.

Schmitz, B., Harper, D.A.T., Peucker-Ehrenbrink, B., Stouge, S., Alwmark, C., Cronholm, A., Bergstrom, S.M., Tassinari, M., Xiaofeng, W., 2008. Asteroid breakup linked to the Great Ordovician Biodiversification Event. Nat Geosci 1, 49–53.

Schmitz, B., Schmieder, M., Liao, S., Martin, E., Terfelt, F., 2022. Impact-crater ages and micrometeorite paleofluxes compared: evidence for the importance of ordinary chondrites in the flux of meteorites and asteroids to Earth over the past 500 million years. In: Koeberl, C., Claeys, P., Montanari, A. (Eds.), From the Guajira Desert to the Apennines, and from Mediterranean Microplates to the Mexican Killer Asteroid: Honoring the Career of Walter Alvarez. Geological Society of America, p. 0.

Schmitz, B., Tassinari, M., Peucker-Ehrenbrink, B., 2001. A rain of ordinary chondritic meteorites in the early Ordovician. Earth Planet Sci Lett 194, 1–15.

Schmitz, B., Yin, Q., Sanborn, M., Tassinari, M., Caplan, C.E., Huss, G.R., 2016. A new type of solar-system material recovered from Ordovician marine limestone. Nat Commun 7 ncomms11851.

Schultz, P.H., Lutz-Garihan, A.B., 1982. Grazing impacts on Mars: a record of lost satellites. J Geophys Res 87, A84–A96.

Scotese, C.R., 2016. PALEOMAP PaleoAtlas for GPlates and the PaleoData Plotter Program. See. http://www.earthbyte.org/paleomap-paleoatlas-for-gplates.

Scotese, C.R., 2021. An atlas of Phanerozoic paleogeographic maps: the seas come in and the seas go out. Annu Rev Earth Planet Sci 49, 679–728.

Terfelt, F., Schmitz, B., 2021. Asteroid break-ups and meteorite delivery to Earth the past 500 million years. Proc Natl Acad Sci USA 118, e2020977118.

Tiscareno, M.S., Hedman, M.M., 2014. Planetary Rings. In: Spohn, T., Breuer, D., Johnson, T. (Eds.), Encyclopedia of the Solar system. ProQuest, pp. 883–905.

Torsvik, T.H., Cocks, L.R.M., 2016. Earth History and Palaeogeography. Cambridge University Press.

Torsvik, T.H., van der Voo, R., Doubrovine, P.V., Burke, K., Steinberger, B., Ashwal, L.D., Trønnes, R.G., Webb, S.J., Bull, A.L., 2014. Deep mantle structure as a reference frame for movements in and on the Earth. Proc Natl Acad Sci USA 111, 8735–8740.

Vokrouhlický, D., Milani, A., Chesley, S.R., 2000. Yarkovsky effect on small near-earth asteroids: mathematical formulation and examples. Icarus 148, 118–138.

Williams, I.P., 2003. The Roche Limit. Celest Mech Dyn Astron 87, 13–25.

Zahnle, K., MacLow, M.M., 1994. The collision of Jupiter and comet Shoemaker-Levy 9. Icarus 108, 1–17.